Effect of chemical and thermal activation on the microstructural and mechanical properties of more sustainable UHPC

Omar Abdulkareem, Amor Ben Fraj, Marwen Bouasker, Abdelhafid Khelidj

Effect of chemical and thermal activation on the microstructural and mechanical properties of more sustainable UHPC

Omar M. Abdulkareem [a,b,c], Amor Ben Fraj [a,*], Marwen Bouasker [d], Abdelhafid Khelidj [b]

[a] *Cerema, Project-team DIMA, 120 rue de Paris, 77171 Sourdun, France*
[b] *Lunam University, University of Nantes, IUT Saint-Nazaire, GeM, UMR CNRS 6183, 58 rue Michel Ange, BP 420-44600, Saint-Nazaire, France*
[c] *University of Mosul, College of Engineering, Department of Environmental Engineering, 41002 Mosul, Iraq*
[d] *University of Orléans, University of Tours, INSA Centre Val de Loire, LaMé, 8 rue Léonard de Vinci, 45072 Orléans, France*

This paper investigates the influence of the content of blast furnace slag (BFS) on the microstructural and mechanical properties of non-activated and activated ultra-high performance concrete (UHPC). Three volume-substitution rates of cement with BFS were explored (30% for $UHPC_2$, 50% for $UHPC_3$ and 80% for $UHPC_4$) and two activation methods, chemical and thermal, were tested. Results show that with 30% of BFS, heterogeneous nucleation prevailed over dilution, accelerating the hydration reaction of cement and increasing the amount of C-S-H formed. C-S-H decreased the porosity of $UHPC_2$ by 18% and 20% respectively at 3 and 90 days. The compressive strengths of $UHPC_1$ (without BFS) and $UHPC_2$ were very similar. For high BFS contents, the dilution effect prevailed and there was less portlandite, which decreased the amount of hydrated products, particularly at early age. As a result, the porosity of $UHPC_3$ and $UHPC_4$ was more than twofold higher than that of $UHPC_1$.

To boost the hydration reaction of blended UHPC with a high BFS content, KOH was added. The use of $[KOH]_3$ significantly increased the amount of hydrated products, reducing the porosity of $UHPC_4$ 1.6-fold at 3 days and increasing its compressive strength by 42% at the same age. However, this activation mode was not enough to ensure the required compressive strength of $UHPC_1$. Thermal activation at 90 °C for 2 days was therefore tested. Results showed the acceleration of the reaction of solid components, which increased the consumption of portlandite and hence the development of hydrated products. This resulted in improving the packing density of blended UHPC, decreasing its porosity and enhancing its compressive strength. In comparison with reference concrete at 90 days, the compressive strength of $UHPC_3$-T increased by 7% and that of $UHPC_4$ was 12.5% lower.

1. Introduction

Since the 1980s, specialized applications that demand greater strength and corrosion resistance triggered research to develop a concrete with an extremely high strength and dense microstructure [1], that subsequently led to the development of ultra-high performance concrete (UHPC). Ultra-high performance concrete is a distinctive cement-based substance that behaves like a minimal-porosity ceramic material with enhanced mechanical properties [2]. This concrete is distinguished by a grain size of the ingredients (cement, silica fume, crushed quartz, quartz sand) that does not exceed 600 μm, a low water-to-binder ratio (w/b) and a high content of water reducer (superplasticizer) [3]. By virtue

* Corresponding author.
E-mail address: amor.ben-fraj@cerema.fr (A. Ben Fraj).

of both the highly dense (specific gravity ranges over 2500–3000 kg/m^3) and homogenous microstructure of UHPC, its typical strength can reach 150–200 MPa in compression, 7–15 MPa in uniaxial tension, and 25–40 MPa in bending [4,5]. This exceptional performance is due to its higher cement content, lower w/b, integration of silica fume and low CaO/SiO_2 ratio [6]. On account of its extraordinary compressive strength, UHPC exhibits great sensitivity to certain parameters such as the quality of cementitious composites, quality of curing (standard or heat treatment), particle size of aggregate and the applied production techniques, etc. Richard and Cheyrezy [7] reported that if soft cast and cured at ambient conditions, its compressive strength (CS) can reach 200 MPa, and that CS values exceeding 800 MPa can be attained when pressure molding is adopted. Hence, the weight of a structure built solely with UHPC can be reduced by one-third to one-half in comparison to that with a traditional reinforced concrete structure under the same load [2,8]. Mounanga et al. [9] ascribed this improvement in mechanical behavior to a better cement hydration and a close granular packing of the UHPC with the addition of crushed quartz. Crushed quartz particles have a high specific area, which improves the homogeneity and the packing density of concrete. From the porosity standpoint the collateral effect of hydration on porosity is as follows: due to the low w/c, the capillary porosity decreases and the Interface Transition Zone (ITZ) is filled up with C–S–H hydrates generated by the pozzolanic reaction of silica fume [10]. The pore size of UHPC essentially ranges between 2 and 3 nm, the most frequent pore size being 2.0 nm, and its total porosity is 2.23% [11].

Despite the high mechanical performance of UHPC, its manufacture involves a high energy consumption. The energy required for cement production is around 1700–1800 MJ t clinker, which is the third largest consumed energy, after that of the aluminum and steel manufacturing industries [12]. The high quantity of cement in UHPC (over 800–1000 kg/m^3) has a detrimental impact on the hydration heat and may create shrinkage deformations, which decrease the hardened performance by microcracking. Besides, it displays downsides from the economic and sustainability standpoints [13].

Portland cement is responsible for 74–81% of global CO_2 release as each 1 kg of cement produced generates around of 0.9 kg of CO_2. This equates to about 3.24 billion tons of CO_2 yearly [12]. Taking into consideration both the boosted mechanical properties of UHPC and its high environmental influence, it appears worthwhile exploring a path to produce UHPC with a low environmental footprint.

Blast furnace slag (BFS) is one of the industrial co-products that can substitute for Portland cement to a certain extent. The use of this alternative material depends mainly on the availability and the domain of application [14]. The major components of BFS are CaO, SiO_2, Al_2O_3 and MgO. It is categorized as a potential hydraulic material (reaction with water) rather than a pozzolanic one (reaction with lime), despite its slow reaction with water [15,16]. This latent hydration reaction restricts the strength development of concrete at early age. However, at later age, the microstructure is more refined, porosity is lower and consequently the mechanical performance of blended concrete is enhanced, in comparison with that of Portland cement. Thanks to its high specific area and its chemical composition, BFS has a double effect on the behavior of UHPC, both physical and chemical. The physical effect consists in (i) the dilution induced by the substitution of cement with BFS, which increases the water-to-cement ratio; (ii) the filler impact due to the fineness of BFS particles, improving the packing density of the mixture; (iii) the stimulation effect, as the BFS particles act as nucleation sites, accelerating the cement hydration reaction [17]. This results in the production of portlandite, which reacts with BFS to form hydrates.

Yu et al. [18] revealed that in presence of slag, the portlandite content of UHPC decreased, denoting its consumption by BFS to form dense C-S-H. The latter fills the pore structure, which results in a compressive strength enhancement of blended UHPC. Other studies have found that increasing the BFS content (70%) increases the portlandite consumption [19] without improving the concrete performance. Zhou et al. [20] observed that the higher the quantity of slag, the higher the total porosity. This can be explained by the very low cement content, which restricts the formation of portlandite. The latter is responsible for promoting the hydration reaction of BFS.

The decrease in mechanical performance of slag-blended UHPC particularly concerns the early age, as the strength development is decelerated by the latent reaction of BFS. Yazici et al. [21] measured a higher drop of compressive strength at 2 days when the slag replacement rate reached 40%, while at 28 days the compressive strength was close to that of reference UHPC. Gupta [22] reported a decrease in early compressive and flexural strengths with 40 and 60% of slag, whereas a growth in later strength was measured even with 80% of slag content. Shi et al. [23] also found that at 3 days, the compressive strength of UHPC decreased from 84 MPa to 78 MPa when 25% of cement was substituted with slag. At 56 days, the compressive strength reached 125 MPa.

Accordingly, since slag itself is nothing more than a latent hydraulic binder with lower early strength and longer setting time, its hydration reaction needs to be boosted. This can be achieved by chemical or thermal activation. Among chemically activated binder systems, alkali activated slag (AAS) is one of the most widespread substances thanks to its lesser environmental effect, quick setting, and swift early strength gain [25]. In presence of an alkali activator (such as sodium or potassium hydroxide), the hydroxyl ions $(OH)^-$ accelerate the hydration reaction by enhancing dissolution of the aluminate and silicate network in the slag to form calcium silicate hydrates with a high amount of Al_2O_3 (C-A-S-H). This increases the early compressive strength [24–26], depending on different factors such as the activator dosage and the interactions between constituents [25,27–29].

As already mentioned, chemical activation is used with ordinary cementitious materials and there has been no research into its effect on UHPC properties. Some research has been carried out, however, on thermally-activated UHPC, mainly in presence of mineral admixtures. Slag, thanks to its higher activation energy, is particularly sensitive to thermal activation [30–32] which accelerates the pozzolanic reaction, increasing the amount of hydrated products and densifying the microstructure even further. As a result, the compressive and flexure tensile strengths will be higher [1,33]. Bougara et al. [34] measured an increase in compressive strength at early age for mixtures with 30% and 50% of slag when the temperature rose from 20 °C to 40 °C and 60 °C, whereas the strength at later age decreased. The same trend was observed by Castellano et al. [35], who measured a great increase in early compressive strength when the temperature was raised from 20 °C to 40 and then to 60 °C. After 7 days the trend was reversed. On the contrary, Sajedi et al. [31] showed that the 90-day compressive strength of mortar with 50% of slag, treated at 60 °C for 20 h, exceeded that of reference mortar by circa 12%.

In conclusion, despite the various studies carried out on UHPC, none have dealt with chemical activation and its effect on UHPC properties, and few of them correlate the thermal activation with the microstructural change, in order to explain the mechanical behavior of UHPC, particularly in presence of slag.

2. Research objective

This paper deals with the effect of BFS content on the microstructural and mechanical properties of non-activated and activated UHPC. The research was carried out at two scales: the

micro-scale, by (i) assessing the different phases resulting from the hydration reaction, and (ii) assessing the porosity, and the macro-scale, by studying the mechanical properties of manufactured UHPC. To highlight the latent reaction of BFS and the interest of chemical and thermal activation in improving blended-UHPC properties, the mechanical properties were measured at 3 and 90 days, and the results were correlated with the state of the microstructure at the same ages.

3. Experimental program

3.1. Materials and mixtures

The materials used to manufacture the concrete were of local origin (France): the cement CEM I 52.5 PM ES comes from Le Teil plant, the grey Silica Fume (SF) is marketed by Condensil as S95 B DM, the Blast Furnace Slag (BFS) comes from Ecocem, the Crushed Quartz (CQ) and Quartz Sand (QS) are marketed by Sibelco as C500 and CV32, respectively. The chemical properties of these components are detailed in [36]. Their physical properties are presented in Table 1.

To ensure the high workability of manufactured UHPC, a Sika Viscocrete Krono HE 20 superplasticizer (SP) was added. It is a high-range water reducer with a density and solid content of 1.085 and 41%, respectively. The content of this acrylic copolymer was adjusted to ensure the same slump flow for all UHPC regardless of their BFS content. All formulations had the same water content (considering the water brought by the superplasticizer) and only BFS and SP contents were varied (Table 2). The optimization of these concrete mixtures is detailed in [36].

Solid components were incorporated in an intensive 15 L Eirich mixer and mixed for 30 s. Then dissolved superplasticizer and water were added and mixed with the other materials for 3 min to ensure a homogeneous mixture, except for UHPC with KOH. For the latter, the mixing time was extended by 30 s to ensure the required slump flow. After mixing, the concrete was poured into steel molds, stored for 24 h before demolding, and plastic-wrapped, to avoid any drying. Subsequently, the specimens were stored in a fog room at 20 °C for 3, 7, 28, and 90 days.

3.2. Methods

3.2.1. Chemical activation

The use of mineral additions, in particular BFS, decelerates the hydration kinetic of concrete and induces a decrease in its early age properties, as the substitution of cement decreases the alkali content of concrete. Alkalis promote the reaction of BFS by destroying its chemical bonds and accelerating its reaction with water, thereby increasing its strength. To compensate for this lack of alkalis, KOH can be added, but its addition may have a negative effect on the environment and should be strictly controlled.

Considering the quantity of alkalis in cement (0.24%), we calculated the quantity of alkalis lost when cement is substituted with BFS and then the quantity of KOH required to compensate for these lost alkalis. This first concentration is called $[KOH]_1$ and equals 3.39 kg/m^3 (3.39 g/l of concrete). This concentration was then increased two ($[KOH]_2$) and three ($[KOH]_3$) times to improve the early age compressive strength of UHPC, without affecting its workability, by maintaining a slump flow of 300 mm. The optimization of this concentration is detailed in [36].

3.2.2. Thermal activation

Thermal activation is employed to accelerate the maturing of concrete, for an equivalent age. The latter corresponds to $t_T = t_x - t_{0,}$ where t_0 and t_x are respectively the time of water/binder contact and the theoretical time to obtain the same level of concrete maturity in the case of conservation at 20 °C.

Generally, the level of maturity depends on hydration reactions and their rate of progress (ξ). The evolution of ξ versus temperature was approximated with Arrhenius' law, applied on all the hydration reactions of cement [37]:

$$\xi = \frac{d\xi}{dt} = \tilde{A}(\xi)\exp\left(-\frac{E_a}{RT}\right) \quad (1)$$

where $\tilde{A}$ is the chemical affinity, ξ the rate of progress of hydration reactions, E_a the activation energy (J mol^{-1}), R the perfect gas constant (8.314 J mol^{-1} K^{-1}) and T the temperature of the concrete throughout the test.

To estimate the equivalent age t_T for moderate thermal treatments, equation 1 was integrated between initial ($t_{initial}$) and final (t_{final}) times, as:

$$t_T = \int_{t_{initial}}^{t_{final}} \exp\left[\frac{E_a}{R}\left(\frac{1}{293}-\frac{1}{T(t)}\right)\right]\cdot dt \quad (2)$$

t_T was approximated as:

$$t_T = \sum_{i=1}^{n}\Delta t_i \cdot \exp\left[\frac{E_a}{R}\left(\frac{1}{293}-\frac{1}{T(t)}\right)\right] \quad (3)$$

where t_T is the equivalent age for the chosen temperature; Δti, the duration of concrete exposure to T_i; Ti, the temperature of concrete during Δti, in Kelvin; E_a, the activation energy and R, the perfect gas constant.

For simplification, E_a is considered as constant and resulting from all the hydration reactions of the binder; E_a/R is 4000 K and 6000 K for CEM I and CEM III, respectively [38,39]. For this study, a high BFS content was explored (up to 62% of whole binder). Thus, the binder was assimilated to composed cement, CEM III. Thermal activation was applied particularly to concretes with a high BFS content ($UHPC_3$ and $UHPC_4$) in order to ensure the same long term properties as $UHPC_1$. Therefore, the equivalent age should be more than 90 days. As shown in Fig. 1, a temperature of 90 °C was applied, 24 h after mixing, for 2 days, before testing UHPC. This results in activated UHPC, with an equivalent age of 103 days.

3.2.3. Thermogravimetric analysis

This test used a thermal analyzer instrument NETZSCH STA 449 F_3 under dynamic nitrogen atmosphere and carried out on 250 mg powdered samples heated from 30 °C to 1250 °C at a rate of 10 °C/min. At a testing age of 3 and 90 days, the specimens were crushed (<315 μm) and hydration was stopped by immersion in methanol. The outputs of the test are the loss in mass per degree Celsius and

Table 1
Fineness and density of solid components.

	CEM I 52.5	SF	QQ	BFS	QS
Specific area (cm^2/g)	3555*	250,000**	10,435*	4450*	124*
Density (–)	3.17	2.24	2.65	2.90	2.65

* Blaine.
** BET.

Table 2
Composition of studied UHPC mixtures.

Components (kg/m^3)	$UHPC_1$	$UHPC_2$	$UHPC_3$	$UHPC_4$	$UHPC_4$-$[KOH]_3$
CEM I	977.00	683.90	488.50	195.40	195.40
SF	183.00	183.00	183.00	183.00	183.00
QQ	61.00	61.00	61.00	61.00	61.00
BFS	–	268.10	446.90	715.00	715.00
QS	1075.00	1075.00	1075.00	1075.00	1075.00
SP	25.31	10.54	22.49	25.31	25.31
W	145.63	160.39	148.44	145.63	140.65
KOH	–	–	–	–	10.17
Slump Flow (mm)	300				

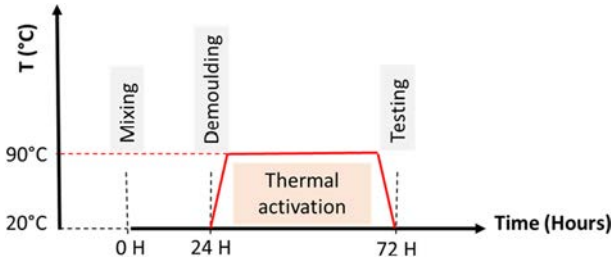

Fig. 1. Thermal activation mechanism.

the differential thermogravimetric (DTG) curves. The mass loss due to the liberation of bound water (H), decomposition of portlandite (CH), and liberation of CO_2 was measured at the respective temperature intervals and the accurate limits for the temperature intervals were specified considering the derivative thermogravimetric curves (DTG). The mass loss of bound water through dehydration of some hydrates (C-S-H, ettringite, etc.) occurred between 180 and 300 °C, while that corresponding to the dehydration of portlandite occurred between 450 and 530 °C. The decarbonation of calcium carbonate took place between 700 and 900 °C.

3.2.4. Total porosity

The Mercury Intrusion Porosimetry (MIP) test was carried out on 1 cm^3 samples at 3 and 90 days. At 3 days, samples were immersed in methanol to stop the hydration reaction, before drying at 105 °C and testing.

3.2.5. Mechanical properties

Flexural and compressive strength tests were carried out on 40 × 40 × 160 mm prism specimens at 3, 7, 28 and 90 days, according to NF EN 196–1. A press machine of 300 kN was used, with loading speeds of 0.05 kN/s and 2.5 kN/s respectively for flexural and compressive tests. Each strength is the average of three samples' strength. The splitting tensile strength was measured on cylindrical specimens 110 mm in diameter by 220 mm in height at 3 and 28 days. The specimens were tested using a 2000 kN-press machine. For each mixture, two cylinders were tested and the mean value is reported.

4. Results and discussion

4.1. Thermogravimetric analysis

The TGA and DTG curves of whole UHPC mixtures after hydrating for 3 and 90 days are presented in Figs. 2–5, respectively. Table 3 shows the variation in content with hydration times of portlandite and calcite beside the amounts of chemically bound water for whole UHPC mixtures.

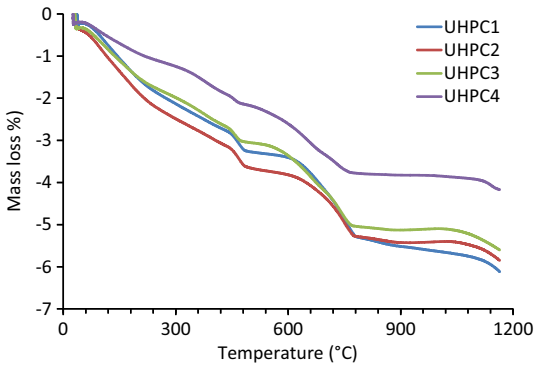

Fig. 2. TGA for UHPC mixtures at 3 days.

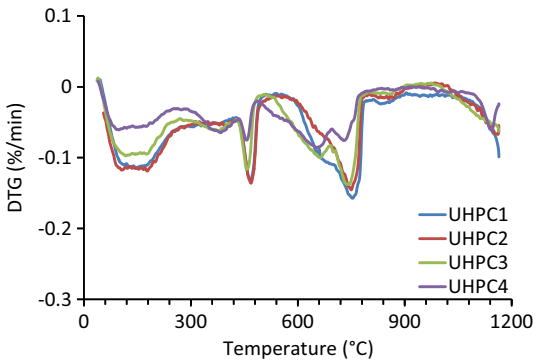

Fig. 3. DTG for UHPC mixtures at 3 days.

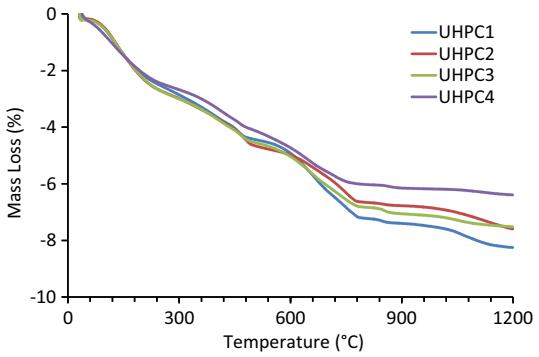

Fig. 4. TGA for UHPC mixtures at 90 days.

4.1.1. Effect of BFS content

The TGA curves of Fig. 2 exhibit the mass loss for the hydrated UHPCs at 3 days, in the following sequential order: dehydration, dehydroxylation or calcination of remaining ettringite, portlandite

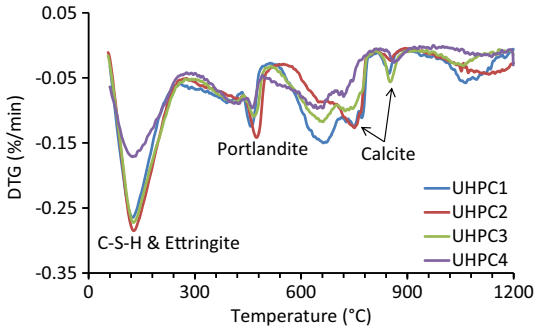

Fig. 5. DTG for UHPC mixtures at 90 days.

decomposition and calcite decarbonation. It can be noted that all the tested specimens demonstrate a comparable trend of mass loss. Nonetheless, the rates of their mass loss in each temperature range are dissimilar, indicating that the quantity of material reacting at each treatment stage differs and depends on the percentage of slag used to substitute for cement, in particular when this reached 80% in $UHPC_4$. The results show that the higher the slag content, the lower the measured mass loss. This can be clearly seen in Table 3 through the difference in mass loss percentages between $UHPC_1$ and $UHPC_4$ at 3 days: the chemically bound water decreased from 3.3 % to 2.1%, portlandite from 1.42% to 0.35%, and calcite from 3.9% to 2.8%, respectively. Generally, the incorporation of slag in cement generates a lower quantity of portlandite in the hydration product due to the impact of dilution in addition to the consumption of portlandite through the pozzolanic reaction [40]. When portlandite forms during cement hydration, some of this compound is consumed by the pozzolanic reaction of silica fume and slag reaction and this consumption is increased when the amount of slag is increased, inducing a delay in concrete hydration and forming supplemental C-S-H [41]. Thus, the mass loss of portlandite in the blended mixtures of UHPC is the least at early ages when compared to $UHPC_1$. Likewise, the results show that the substitution of Portland cement with slag diminishes the quantity of C-S-H and C-A-H formed at 3 days in comparison with $UHPC_1$. The quantification of phases related to mass change for the UHPC mixtures was accompanied by the occurrence of major peaks in the DTG curves, as shown in Fig. 3. The prominence of these peaks can be attributed to the evaporation of free water, portlandite and calcite decompositions, sequentially. The endothermic peak of both C-S-H and ettringite decreases with increasing slag content. The decrease of the portlandite content in the UHPCs containing slag restricts the promotion of the slag pozzolanic reaction, and the already-produced pore structure in these blended mixtures cannot be filled by the recently produced C-S-H.

As expected, the content of chemically bound water in the UHPC mixtures increases remarkably at 90 days, as shown in Table 3. The measured mass loss of the UHPC mixtures also increases with increasing age up to 90 days, indicating a continuing hydration with time as demonstrated in Fig. 4. The mass loss of portlandite remains lower in the UHPC mixtures containing slag compared to $UHPC_1$ since the particular cementitious matrix of UHPC limits the slag pozzolanic reaction to a great extent, with the result that beyond 90 days only a small amount of slag is available to react with portlandite. The data also show that the portlandite consumption in all UHPC mixtures increased with the progress of the hydration age. Compared to the portlandite quantities at 3 days, the mass loss amounts at 90 days were reduced by about 39%, 41%, 21% and 37% for $UHPC_1$, $UHPC_2$, $UHPC_3$ and $UHPC_4$ respectively. The increase in slag content induces a decrease in non-evaporable water on account of the weak hydraulic activity of the slag blended matrix [42]. From Fig. 5, it was observed that the peaks of both C-S-H and ettringite in all UHPC mixtures at 90 days were higher than that at 3 days, indicating an increase in C-S-H at the cost of portlandite because of the pozzolanic reaction [40]. The portlandite peaks of all the blended mixtures of UHPC are lower due to the impact of dilution and the consumption of portlandite by the pozzolanic reaction. In addition, there are different peaks of calcite, as observed in Fig. 5. Some phases such $MgCO_3$, $MnCO_3$ and $FeCO_3$ can decompose at temperatures lower than that of calcite. However, all the curves clearly show the decrease in calcite when the cement content decreases.

4.1.2. Effect of chemical activation

Fig. 6 shows the mass loss for alkali-activated and non-activated $UHPC_4$. This figure highlights the rapid decrease in mass for activated UHPC, at 3 and 90 days, in comparison with that of non-activated ones. The difference is clearly shown in Fig. 7, where the peak corresponding to C-S-H decomposition is particularly high for activated UHPC. At 3 days, a plateau is observed for non-activated $UHPC_4$, denoting a delay in the formation of hydrates, for high BFS content and in the absence of any activator. Using KOH appears to promote the BFS reaction and accelerate the development of hydrates, from early age, as shown in Table 3, for $UHPC_4$-$[KOH]_3$. At 90 days, the measured peaks of C-S-H are practically the same for both activated and non-activated UHPCs.

The activation of $UHPC_4$ increases the chemically bound water twofold at 3 days, denoting an acceleration of the slag reaction, which consumes all the portlandite produced. Thus, the hydration reaction is rapidly stopped, which explains the low content in chemically bound water of $UHPC_4$-$[KOH]_3$ at 90 days, in comparison with the non-activated one.

The results obtained agree with those of hydration [36], where a second peak of heat flow appeared 16 h earlier when KOH was used, corresponding to the reaction of slag.

4.1.3. Effect of thermal activation

In order to obtain the same performances of $UHPC_1$ at 90 days, concretes with high slag content were thermally activated. As expected, a great mass loss was observed, at early age, for

Table 3
Mass loss percentages (%) for reaction products from TGA analysis of UHPC mixtures.

Mixture designation	Chemically bound water		Portlandite		Calcite	
	3 days	90 days	3 days	90 days	3 days	90 days
$UHPC_1$	3.30	4.80	1.42	0.86	3.90	5.30
$UHPC_2$	3.10	4.90	1.35	0.80	3.00	3.30
$UHPC_3$	2.60	4.80	0.93	0.73	2.90	3.00
$UHPC_4$	2.10	4.10	0.35	0.22	2.80	2.50
$UHPC_4$-$[KOH]_3$	4.40	3.80	0.00	0.00	4.20	1.80
$UHPC_3$-T	4.80		0.00		1.20	
$UHPC_4$-T	3.70		0.00		0.20	

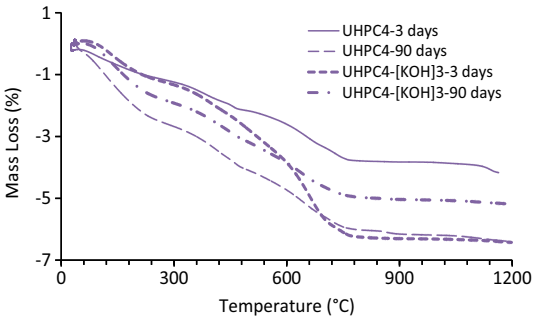

Fig. 6. TGA for $UHPC_4$ mixtures with and without chemical activation.

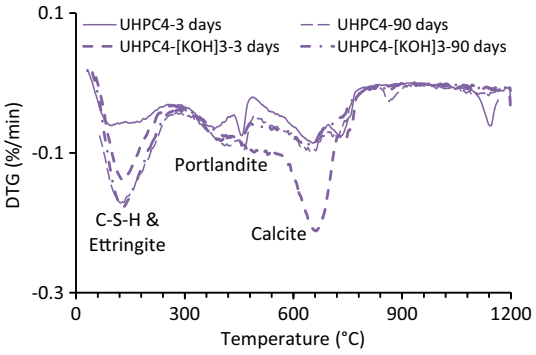

Fig. 7. DTG for $UHPC_4$ mixtures with and without chemical activation.

thermally-activated UHPCs, in comparison with non-activated $UHPC_1$ (see Fig. 8). Later, the curves have a similar trend. Fig. 9 shows that this increase corresponds particularly to the dehydration of C-S-H, as thermal activation promotes cement hydration and the pozzolanic reaction [43]. This results in increasing the C-S-H content of $UHPC_3$ and $UHPC_4$, by circa 6 and 4 times, respectively. $UHPC_3$-T and $UHPC_4$-T contain respectively 4 and 4.6 times more C-S-H than $UHPC_1$. From Table 3, it can be seen that even if the chemically bound water measured is the same for $UHPC_3$-T and $UHPC_1$ (4.8%), that of $UHPC_4$ is lower (3.7%). The high content of slag in the latter affects the hydration progress, despite the application of thermal activation, which could result in a decrease in compressive strength.

As for chemical activation, thermal activation promotes cement and mineral additions reactions, which increase portlandite consumption. Table 3 shows the total consumption of portlandite in $UHPC_3$-T and $UHPC_4$-T and the presence of a small quantity of calcite, proportional to their cement contents.

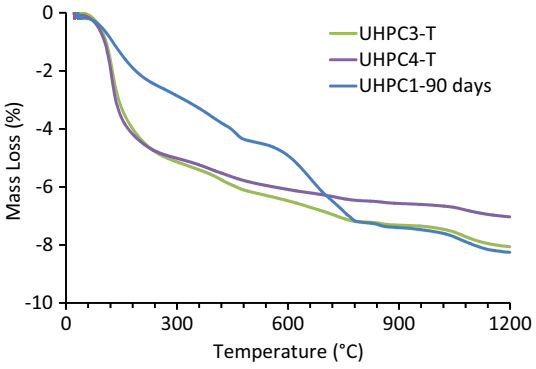

Fig. 8. Comparison of TGA curves for thermally-activated $UHPC_3$ and $UHPC_4$ mixtures with the reference one at 90 days.

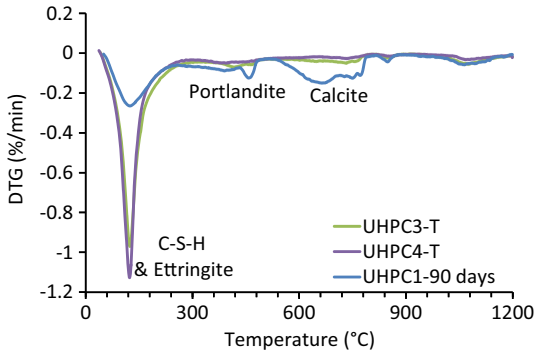

Fig. 9. Comparison of DTG curves for thermally-activated $UHPC_3$ and $UHPC_4$ mixtures with the reference one at 90 days.

4.2. Porosity

The total porosity of each UHPC specimen was measured at 3 and 90 days and analyzed regardless of the slag content and the chemical and thermal activations applied. Results are summarized in Table 4.

4.2.1. Effect of slag content

Table 4 shows that the porosity of $UHPC_1$ is very low (5.45%) even at 3 days. As mentioned earlier, the essential cementitious compound in $UHPC_1$ is silica fume. At larger amounts of silica fume, e.g. 25%, the capillary porosity is low. As a rule, silica fume improves the packing density of UHPC in two ways: i) its filler impact through its finer particles that fill the voids between cement particles and the spaces between cement particles and aggregate, and ii) the pozzolanic impact due to the fact that the silica fume reacts with portlandite to form further C–S–H gel resulting in an additional decrease in both pore diameter and capillary porosity through hydration [44]. For $UHPC_2$, the total porosity dropped by 18% compared to that of $UHPC_1$ at 3 days. The heterogeneous nucleation caused by the fineness of slag particles prevails over the latent reaction of slag, which results in the acceleration of hydration [36] and decreases UHPC porosity. In contrast, when the slag content was high, the total porosity also increased. For $UHPC_3$ and $UHPC_4$, the porosity was enhanced by 1.9 and 2.3 times respectively, in comparison with $UHPC_1$. This increase in the porosity of UHPC specimens cured at 3 days is due to the latent reactivity of slag. The higher slag inclusion increases the porosity of UHPC specimens cured at 3 days on account of the latent reactivity of slag. This decelerates the hydration reaction of blended slag mixtures and postpones the formation of hydrates, which induces an increase in the number of coarse pores and hence in the total porosity [20,45].

At advanced ages the porosity of the blended slag mixture tends to be lower than that of the Portland cement mixture. The reaction

Table 4
Total porosity of UHPC specimens.

Mixture designation	Total porosity (%)	
	3 days	90 days
$UHPC_1$	5.45	4.81
$UHPC_2$	4.47	3.85
$UHPC_3$	10.51	2.51
$UHPC_4$	12.57	4.04
$UHPC_4$-$[KOH]_3$	7.72	4.14
$UHPC_3$-T	2.64	
$UHPC_4$-T	4.09	

of slag and C-S-H fills capillary pores and refines the structure, which increases the fine pores of blended mixtures [46,47].

At 90 days, the total porosity of $UHPC_1$ and $UHPC_2$ decreased by circa 12% and 14%, respectively, in comparison with that at 3 days. For slag contents of 50% and 80%, the porosity decreased by 4 and 3 times, respectively. This result highlights the latent reaction of slag, which has a beneficial effect in the long term. Thus, the slag reaction generates hydration products that fill the large pores continuously at a prolonged hydration age and significantly decreases the concrete porosity [45,48].

4.2.2. Effect of chemical activation

As observed, adding KOH decreases the total porosity of $UHPC_4$ by 39% at 3 days. The porosity measured at 90 days changed slightly. As is well-known, AAS paste has a finer matrix system than cement paste because for the same water-to-binder ratio, the hydration products have more gel pores and the pastes have fewer capillary pores [31]. Several studies have established that when a suitable chemical activator is used, the porosity of alkali-activated slag paste is lower, with smaller pores and a higher proportion of micro pores, while the proportion of capillary pores is less than in Portland cement paste [49–51]. The microstructure evolution of hydrating AAS paste is governed by rapid alterations at early ages, and latent evolution later. This correlates well with the quick setting of the AAS mixture, and its slow strength development at later ages [31,36].

4.2.3. Effect of thermal activation

Table 4 shows that the effect of thermal activation was more pronounced than that of chemical activation on the porosity of the thermally-activated $UHPC_3$ and $UHPC_4$ mixtures at 3 days whereas at 90 days there is no clear impact on the porosity apart from a slight decrease when compared to $UHPC_1$. This was linked with the slag content; the higher the slag content of thermally-activated UHPC, the more porosity decreases. The high temperature accelerates the hydration of cement and significantly promotes the slag reaction during early ages, making the composite binder highly compact. These results agree with the TGA observations, that demonstrate the increase in C-S-H content when UHPCs are thermally activated. These hydrates fill voids, improve the packing density of concrete and greatly decrease its porosity.

4.3. Mechanical properties

In this section, the flexure, compressive and splitting tensile strengths are explored for the different UHPCs studied. The cited parameters were analyzed regardless of BFS content and activation methods, as the mechanical properties of UHPC depend on the curing regime [51].

4.3.1. Effect of slag content

The incorporation of different amounts of slag in blended mixtures of UHPC results in different flexure and compressive strengths, as illustrated by Figs. 10 and 11, respectively.

Figs. 10 and 11 show that the strength gains of $UHPC_2$ in flexion are 6%, 4%, 13% and 4% whereas the gains in compression ratios are 2.8%, 6%, 1.4% and 1.2% for 3, 7, 28 and 90 days respectively. If we focus on compressive strength, we note that the substitution of 30% of cement with BFS induces a pronounced increase at early age (3 and 7 days) in comparison with 28 and 90 days. There are two possible reasons for this result: i) the high superplasticizer dosage of $UHPC_1$, compared to $UHPC_2$, which restricts the hydration reaction of cement particles and delays the formation of hydrates. This results in decreasing compressive strength, particularly at early age (3 days); ii) the beneficial effect of BFS particles on concrete hydration and hardening. This effect, due to the high

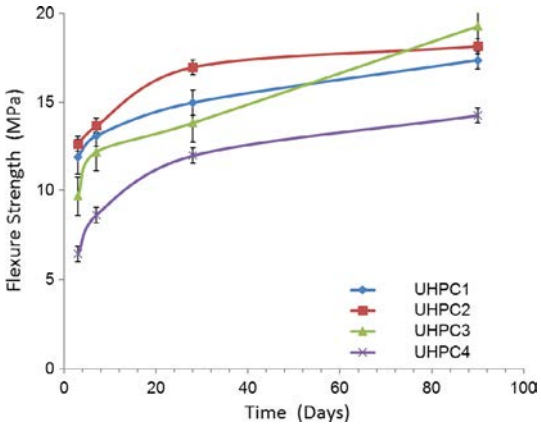

Fig. 10. Flexure strength of studied UHPCs.

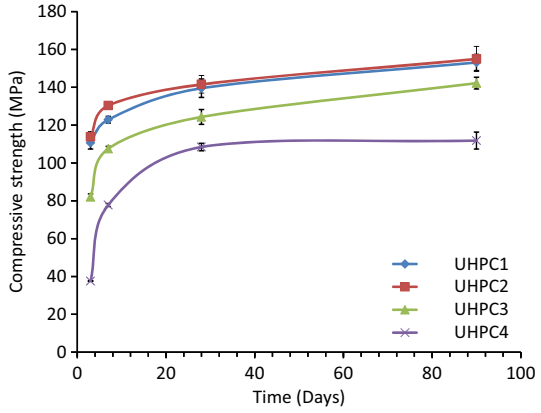

Fig. 11. Compressive strength of studied UHPCs.

specific area of BFS, is twofold: a physical effect, by improving the packing density of UHPC, and a chemical effect by activating the cement hydration. Thanks to their fineness, BFS particles fill voids between cement grains and those between quartz sand ones, which enhances the bond strength between the components of the matrix skeleton [21,52] and intensifies the interfacial transition zone of the aggregate-cement paste. In addition, BFS particles, like SF ones, act as heterogeneous nucleation sites, thereby accelerating the hydration of cement [36] and the formation of hydrates, necessary for strength development. The results are in accordance with those of thermogravimetric analysis. The low density C-S-H gel that is formed fills the capillary pores, thus decreasing the total porosity of $UHPC_2$ by 18% at 3 days, as shown in Table 4.

At later ages (28 and 90 days) the difference between $UHPC_1$ and $UHPC_2$ is reduced, and the compressive strength of the latter slightly exceeds that of the former. This trend can be explained by the low water content of UHPC, which restricts the long-term SF and BFS reactions since, unlike ordinary and high performance concretes, the portlandite formed in UHPC is reduced. As portlandite is necessary for the pozzolanic reaction of SF and BFS, its scarcity decreases their reactivity.

In order to show the *filler* effect of slag in improving packing density and hence the compressive strength of concrete, limestone filler was incorporated as a partial substitution of cement (30%) and the concrete was compared to that with slag. Figs. 12 and 13 show respectively the flexure and compressive strength of $UHPC_2$ based on slag and limestone filler.

Despite its lower specific area, in comparison with limestone filler, slag confers more compressive strength at all curing ages. This

result highlights the slight reactivity of slag at early age, which compensates for the loss of strength that should occur because of decreasing specific area. Limestone filler, despite its high specific area, is considered as an inert mineral material. Its effect consists in increasing the compressive strength at early age by heterogeneous nucleation, while slag could play a complex role consisting in filling voids between cement particles, improving compressive strength by heterogeneous nucleation in addition to its chemical effect through its latent reactivity at early age.

With high BFS content, the decrease in compressive and flexure strengths is significant, particularly at early age. As shown in Fig. 10, the drop in compressive strength of $UHPC_3$ is 26%, 12%, 11% and 7% whereas for $UHPC_4$ it is 66%, 37%, 22% and 27% at 3,7, 28 and 90 days, respectively. As explained in our recent study [36], at early age, the dilution effect of BFS particles prevails over the effect of heterogeneous nucleation. This results in a high liquid–solid ratio, delaying the hardening of UHPC and its strength development. According to thermogravimetric analysis, at 3 days, the rates of hydrates and portlandite formed are very low, denoting the delay of cement hydration and the latent reaction of slag, making the UHPC microstructure more porous and reducing the compressive strength. At later ages (28 and 90 days), the difference between $UHPC_1$ and $UHPC_3$ decreases, denoting the progress of the pozzolonic reaction of SF and BFS. For $UHPC_4$, the compressive strength, despite its rapid increase between 3 and 7 days, is the same at 28 and 90 days. This trend shows that the hydration reaction of solid components is postponed after 28 days and the rate of hydrates formed is low. Indeed, with a high BFS and a low water content, the amount of portlandite produced is limited and is not enough for the pozzolanic reaction of SF and BFS. This reduces the C-S-H content and decreases the compressive strength, despite the refinement of the microstructure [53].

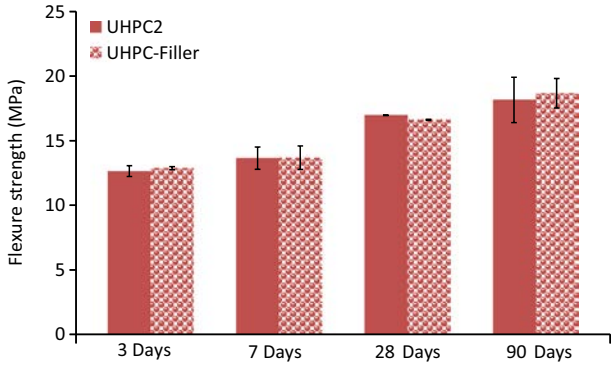

Fig. 12. Flexure strength of $UHPC_2$ with slag and limestone filler.

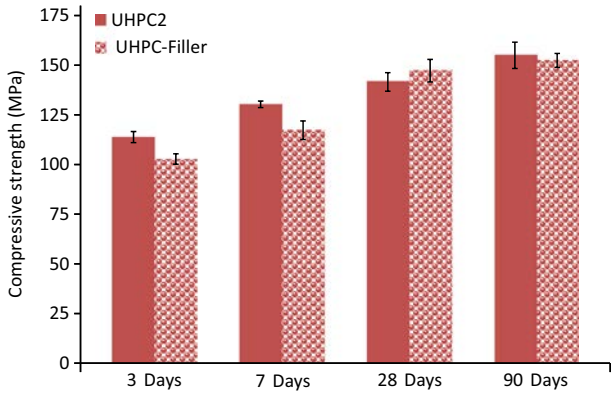

Fig. 13. Compressive strength of $UHPC_2$ with slag and limestone filler.

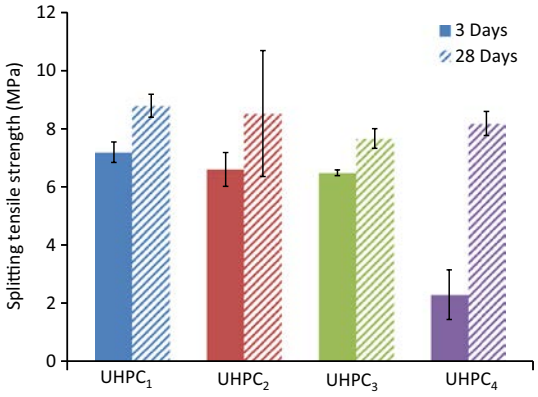

Fig. 14. Splitting tensile strength of studied UHPCs.

Fig. 14 shows the splitting tensile strength of different UHPCs at 3 and 28 days. All the manufactured UHPCs have a splitting tensile strength at 28 days exceeding 8 MPa, despite the absence of fibers. This result is very interesting, as the tensile strength is a key parameter in UHPC mixture design.

Even if a low BFS content does not greatly affect the concrete tensile strength, for 50% of cement substitution a decrease in strength of 10% and 13% was measured at 3 and 28 days, respectively. The drop in tensile strength is particularly pronounced for concrete with 80% of BFS at 3 days, reaching 68%. This result agrees with that of compressive strength.

The same factors influencing the compressive strength of the tested UHPCs are presented below to explain the effect of BFS content on the splitting tensile strength, even if the latter seems less sensitive than the former.

4.3.2. Effect of chemical activation

As mentioned earlier, the original concentration of the alkaline activator used here, $[KOH]_1$, was calculated to compensate for the lack of alkalis caused by the substitution of cement. The concentration of KOH needs to be high to improve the early age properties of blended UHPCs [36]. Therefore, we will focus on $UHPC_4$, where the rate of cement substitution is high. Thus, a large quantity of KOH (proportional to the BFS content) can be added. To ensure the required compressive strength of $UHPC_4$, the concentration of $[KOH]_1$ was increased up three times ($[KOH]_3$). This is considered as the optimal concentration, even if more hydroxide potassium is necessary to improve the early compressive strength of $UHPC_4$, in order to reach that of reference UHPC, since more KOH strongly affects the workability [36] of concrete and has a negative effect on its implementation and then on its compressive strength.

Figs. 15 and 16 depict the variation of both flexure and compressive strengths of KOH-activated UHPCs with 80% slag ($UHPC_4$).

As shown in Fig. 15, the flexure strength increases proportionally to the activator concentration, denoting the regularity and the high density of the interfacial transition zone between the binder and the aggregate in alkali-activated slag mixtures [25]. This was helpful for increasing the bond strength of alkali-activated concretes as in presence of alkalis, BFS particles react rapidly, promoting the formation of hydrates, which explains the high consumption of portlandite for $UHPC_4$-$[KOH]_3$ (Section 4.1.2). The hydrates formed fill the porosity and improve the properties of the transition zone in [KOH]-activated UHPCs. This results in an increase in flexure strength.

Like flexure strength, compressive strength is improved by chemical activation, particularly at early age and with a high concentration of alkaline activator. For $[KOH]_3$, the measured growth of compressive strength was nearly 42% at 3 days whereas at 7,

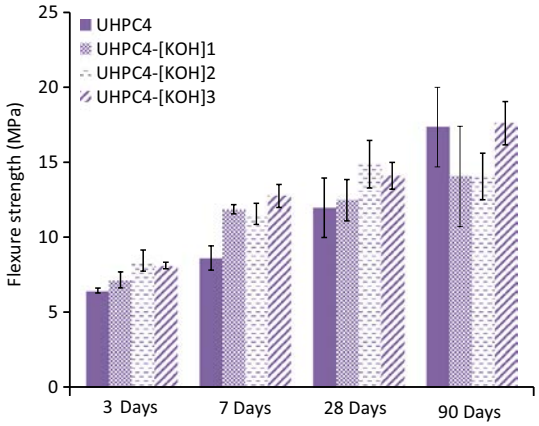

Fig. 15. Flexure strength of KOH-activated $UHPC_4$.

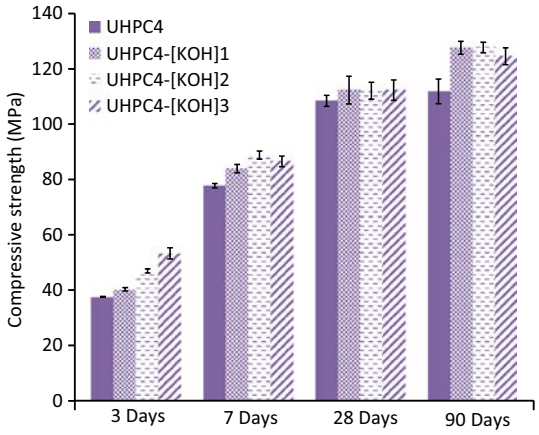

Fig. 16. Compressive strength of KOH-activated $UHPC_4$.

28 and 90 days, the strength gain reached about 14%, 3% and 14%, as shown on Fig. 16. This trend is in accordance with that of previous studies, emphasizing the dosage of activating agent as a paramount factor in improving the early age performance of blended mixtures [54–57].

The presence of a high concentration of KOH increases the solution's pH (i.e. higher alkalinity and correspondingly higher concentration of OH^- ions), which increases the dissolution ability of both Si and Al ions by destroying the Si—O and Al—O bonds in the slag glass matrix. This is followed by the precipitation of hydrated products with low solubility, such as calcium silicates, calcium aluminates, and magnesium aluminate. Then, steady ettringite is formed as a result of the interaction between Ca and Al. As a combined result of rising pH and ettringite formation, hydration is accelerated [36], increasing hydrate formation and improving the compressive strength of concrete at early age [58]. The result obtained agrees with those of thermogravimetric analysis and porosity: the DTG curves clearly show the great increase in C-S-H at 3 days when KOH is added, decreasing the total porosity of $UHPC_4$ by 39%.

4.3.3. Effect of thermal activation

In order to reach the required compressive strength of reference concrete at 90 days, $UHPC_3$ and $UHPC_4$ were thermally-activated. The results of flexure and compressive strengths in comparison with $UHPC_1$ at 90 days are shown in Figs. 17 and 18, respectively.

In comparison with non-activated blended UHPCs, the flexure and compressive strength of both $UHPC_3$-T and $UHPC_4$-T increased substantially. This result shows the important role of thermal activation in accelerating the hydration process and producing hydrates, particularly in presence of BFS and SF, which improves the packing density and decreases the concrete's porosity. This results in increasing the mechanical properties of UHPC.

As observed in Fig. 18, thermal activation increases the compressive strength at 3 days of $UHPC_3$ and $UHPC_4$ by 1.7 and 3 times, respectively. The temperature accelerates the reaction of the solid components of concrete, particularly BFS. Thus, the higher the amount of slag, the higher the apparent hydration activation energy [31,32]. At 90 days, the compressive strength increase is circa 16% and 20% respectively for $UHPC_3$ and $UHPC_4$. This result shows that contrary to ordinary and high performance concretes, thermal activation improves the mechanical properties of UHPC at later age. For the former with thermal activation, there is not enough time for hydrated products to be regularly arranged inside the pores of the hardened paste, which enlarges the capillary pores and then decreases the later strength. This phenomenon is known as crossover impact [33,35]. For UHPC, there is not enough water for complete concrete hydration, which enables the development of compressive strength at later age. Therefore, the high temperature compensates for the lack of water, by activating the solid components, particularly the more sensitive ones (BFS). This results in a high consumption of portlandite (0% for thermally-activated UHPC) by mineral admixtures [59], inducing a high production of hydrates which fill the pores and improve the packing density of UHPC. The porosity drops and the compressive strength increases.

As already mentioned, the objective of thermal activation is to reach the compressive strength of $UHPC_1$ at 90 days. This objective was reached for $UHPC_3$ and its compressive strength exceeded that of reference concrete by 7%, denoting the effectiveness of the activation mode applied (temperature and duration). For $UHPC_4$, thermal activation improved the compressive strength but without reaching that of reference concrete (-12.5%) as the low cement content combined with the high water absorption of SF and BFS strongly affect the compressive strength, and thermal activation at 90 °C for 48 h did not counterbalance this drop. Therefore, the temperature should be increased or the duration should be extended to compensate for the decrease in compressive strength in presence of a high BFS content. However, the environmental footprint of this activated UHPC has to be assessed, despite its low cement content. Another activation mode, without increasing temperature or duration, could be investigated, combining chemical and thermal activation.

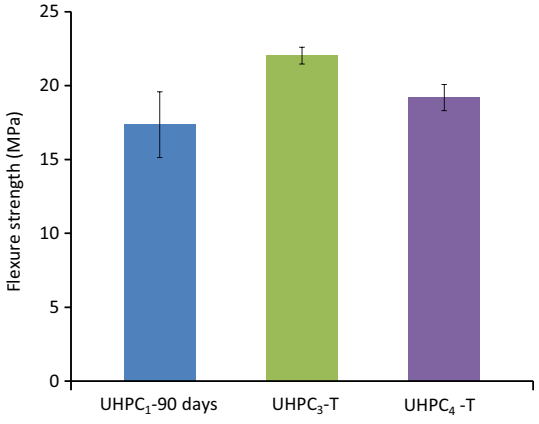

Fig. 17. Comparison of flexure strengths of thermally-activated $UHPC_3$ and $UHPC_4$ with $UHPC_1$.

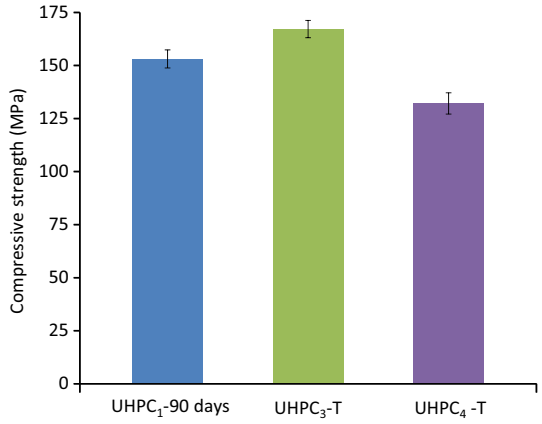

Fig. 18. Comparison of compressive strengths of thermally-activated $UHPC_3$ and $UHPC_4$ with $UHPC_1$.

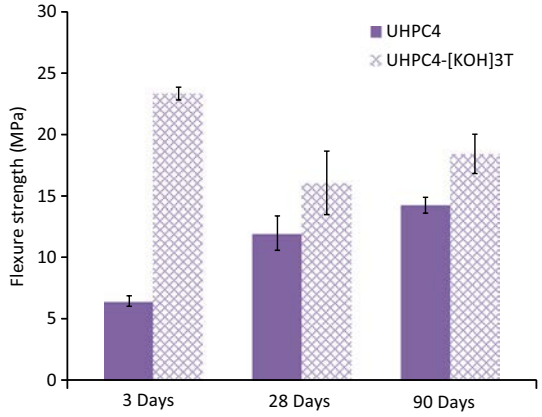

Fig. 19. Flexure strength of chemically and thermally-activated $UHPC_4$ mixtures.

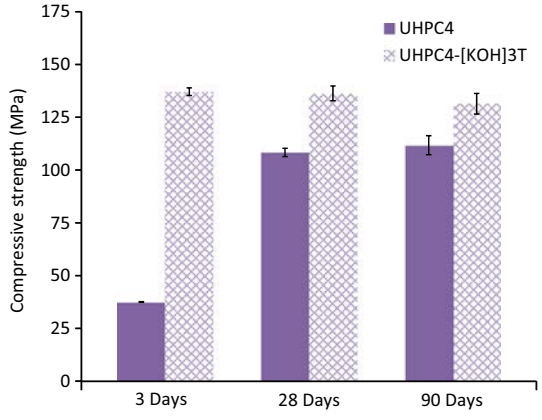

Fig. 20. Compressive strength of chemically and thermally-activated $UHPC_4$ mixtures.

4.3.4. Effect of combined chemical and thermal activation

The combined activation mode consists in using chemical and thermal activation sequentially. In our case, $UHPC_4$-$[KOH]_3$ was demolded after 24 h and thermally-activated for 48 h, as detailed previously. The results of flexure and compressive strengths at 3, 28 and 90 days are shown in Figs. 19 and 20, respectively.

Figs. 19 and 20 show clearly that the effect of chemical activation with $[KOH]_3$ is negligible, as the measured compressive strength does not exceed that of $UHPC_4$-T. This result highlights two interesting points: i) even if $[KOH]_3$ improves the compressive strength of $UHPC_4$ at 3 days, this improvement is negligible at 1 day, as the concrete has a high superplasticizer content, which decelerates the hydration reaction of cement and hence that of activated slag; ii) thermal activation, applied at 1 day, ensures an activation of all silicon solid components, which accelerates their hydration reaction and induces a pronounced increase in strength. In addition, the hydrates formed in thermally-activated UHPC are denser than those formed with chemical activation. Therefore, in our case study, it is not interesting to combine chemical and thermal activation.

5. Conclusions

The work carried out allows us to draw the following conclusions:

- With 30% of slag, the heterogeneous nucleation effect of BFS particles prevails over the effect of dilution. This results in an acceleration of the cement hydration reaction and consequently that of mineral admixtures (SF and BFS), which increases the amount of hydrates produced. The latter improve the packing density of concrete and decrease its porosity. Therefore, the compressive strength increases.
  In addition to the compressive strength enhancement, BFS particles improve the UHPC workability by their filling and lubrication roles, which decreases the superplasticizer content. This reduces the environmental impact and the cost of $UHPC_2$ in comparison with $UHPC_1$.
- For high BFS content (50% and 80%), the dilution effect prevails over the heterogeneous nucleation effect. The compressive strength of $UHPC_3$ and $UHPC_4$ increased slightly, denoting the low portlandite content, which results in fewer hydrates. Despite the physical effect (filling pores and improving the packing density) of BFS, the lack of water and portlandite restrict the pozzolanic reaction of SF and BFS, which decreases the mechanical performance of blended UHPC in comparison with the reference one.
- Alkaline activation with $[KOH]_3$ increases the dissolution of Si and Al ions by breaking the Si—O and Al—O bonds in the slag glass, which promotes the BFS reaction. This increases the amount of C-S-H, decreasing porosity and improving the compressive strength of $UHPC_4$ at early age.
- Thermal activation increases the reaction of solid components and accelerates their hydration, which increases the consumption of portlandite. Therefore, more hydrates are formed, filling the porosity, improving the packing density of UHPC and enhancing its mechanical performance. For $UHPC_3$-T, the thermal activation parameters chosen ensured the required compressive strength. However, with 90 °C and 48 h of activation, the compressive strength of $UHPC_4$-T was 12.5% less than that of $UHPC_1$ at 90 days, due to the lack of water and the high BFS content. In order to improve the compressive strength of $UHPC_4$, higher temperatures or longer durations have to be explored, as the combined chemical and thermal activation was not enough to compensate for the drop in strength.

Acknowledgment

The authors would like to address their thanks to Jérôme Carriat for his technical help in manufacturing and characterizing the concretes.

References

[1] E. Fehling, M. Schmidt, J. Walraven, T. Leutbecher, S. Fröhlich, Ultra-high performance concrete UHPC: Fundamentals-Design-Examples, Wilhelm Ernst & Sohn, 10245 Berlin, Germany, 2014.

[2] V. Corinaldesi, G. Moriconi, Mechanical and thermal evaluation of ultra high performance fiber reinforced concretes for engineering applications, Constr. Build. Mater. 26 (2012) 289–294.

[3] M. Laneza, M.N. Oudjita, A. Zenatia, K. Arroudj, A. Bali, Micro Environ. Concr. Phys. Proced. 21 (2011) 159–165.

[4] M.A.A. Aldahdooh, N.M. Bunnori, M.A.M. Johari, Influence of palm oil fuel ash on ultimate flexural and uniaxial tensile strength of green ultra-high performance fiber reinforced cementitious composites, Mater. Des. 54 (2014) 694–701.

[5] D. Mostofinejad, M.R. Nikoo, S.A. Hosseini, Determination of optimized mix design and curing conditions of reactive powder concrete (RPC), Constr. Build. Mater. 123 (2016) 754–767.

[6] A. Beglarigale, H. Yazıcı, Pull-out behavior of steel fiber embedded in flowable RPC and ordinary mortar, Constr. Build. Mater. 75 (2015) 255–265.

[7] P. Richard, M. Cheyrezy, Composition of reactive powder concretes, Cem. Concr. Res. 25 (1995) 1501–1511.

[8] D.-Y. Yoo, N. Banthia, Mechanical properties of ultra-high-performance fiber-reinforced concrete: a review, Cem. Concr. Compos. 73 (2016) 267–280.

[9] P. Mounanga, K. Cherkaoui, A. Khelidj, M. Courtial, M.-N. de Noirfontaine, F. Dunstetter, Extrudable Reactive Powder Concretes: Hydration, shrinkage and transfer properties. Europ. J. Environ. Civ. Eng. 16 (1) (2012) 1–20.

[10] M. Courtial, M.-N. de Noirfontaine, F. Dunstetter, M. Signes-Frehel, P. Mounanga, K. Cherkaoui, A. Khelidj, Effect of polycarboxylate and crushed quartz in UHPC: microstructural investigation, Constr. Build. Mater. 44 (2013) 699–705.

[11] D. Wang, C. Shi, Z. Wu, J. Xiao, Z. Huang, Z. Fang, A review on ultra high performance concrete: Part II. Hydration, microstructure and properties, Constr. Build. Mater. 96 (2015) 368–377.

[12] A.M. Rashad, D.M. Sadek, H.A. Hassan, An investigation on blast-furnace slag as fine aggregate in alkali-activated slag mortars subjected to elevated temperatures, J. Clean. Prod. 112 (2016) 1086–1096.

[13] H. Yazıcı, H. Yiğiter, A.Ş. Karabulut, B. Baradan, Utilization of fly ash and ground granulated blast furnace slag as an alternative silica source in reactive powder concrete, Fuel 87 (2008) 2401–2407.

[14] E. Aprianti, P. Shafigh, R. Zawawi, Z.F. Abu, Hassan, introducing an effective curing method for mortar containing high volume cementitious materials, Constr. Build. Mater. 107 (2016) 365–377.

[15] F. Sajedi, Effect of curing regime and temperature on the compressive strength of cement-slag mortars, Constr. Build. Mater. 36 (2012) 549–556.

[16] C. Li, H. Sun, L. Li, A review: The comparison between alkali-activated slag (Si +Ca) and metakaolin (Si+Al) cements, Cem. Concr. Res. 40 (2010) 1341–1349.

[17] P. Lawrence, M. Cyr, E. Ringot, Mineral admixtures in mortars. Effect of inert materials on short-term hydration, Cem. Concr. Res. 33 (2003) 1939–1947.

[18] R. Yu, P. Spiesz, H.J.H. Brouwers, Development of an eco-friendly Ultra-High Performance Concrete (UHPC) with efficient cement and mineral admixtures uses, Cem. Concr. Compos. 55 (2015) 383–394.

[19] P.E. Holthuizen, Chloride ingress of carbonated blast furnace slag cement mortars, Section of Materials and Environment (Master Thesis), Delft University of Technology, Netherlands, 2016.

[20] J. Zhou, G. Ye, K. van Breugel, Hydration process and pore structure of portland cement paste blended with blast furnace slag, in: Proceedings of the 6th International Symposium on Cement & Concrete, Canmet, 2006, pp. 1–7.

[21] H. Yazıcı, M.Y. Yardımcı, S. Aydın, A.S. Karabulut, Mechanical properties of reactive powder concrete containing mineral admixtures under different curing regimes, Constr. Build. Mater. 23 (2009) 1223–1231.

[22] S. Gupta, Development of ultra-high performance concrete incorporating blend of slag and silica fume as cement replacement, Int. J. Civ. Struct. Eng. Res. 2 (1) (2014) 35–51.

[23] C. Shi, D. Wang, L. Wu, Z. Wu, The hydration and microstructure of ultra-high-strength concrete with cement–silica fume–slag binder, Cem. Concr. Compos. 61 (2015) 44–52.

[24] S.A. Bernal, R. Mejía de Gutiérrez, A.L. Pedraza, J.L. Provis, E.D. Rodriguez, S. Delvasto, Effect of binder content on the performance of alkali-activated slag concretes, Cem. Concr. Res. 41 (2011) 1–8.

[25] F. Sajedi, H. Abdul Razak, The effect of chemical activators on early strength of ordinary Portland cement-slag mortars, Constr. Build. Mater. 24 (2010) 1944–1951.

[26] X. Wu, W. Jiang, D.M. Roy, Early activation and properties of slag cement, Cem. Concr. Res. 20 (1990) 961–974.

[27] M. Kovtun, E.P. Kearsley, J. Shekhovtsova, Chemical acceleration of a neutral granulated blast-furnace slag activated by sodium carbonate, Cem. Concr. Res. 72 (2015) 1–9.

[28] B.S. Gebregziabiher, R. Thomas, S. Peethamparan, Very early-age reaction kinetics and microstructural development in alkali-activated slag, Cem. Concr. Compos. 55 (2015) 91–102.

[29] E. Altan, S.T. Erdoğan, Alkali activation of a slag at ambient and elevated temperatures, Cem. Concr. Compos. 34 (2012) 131–139.

[30] W. Chen, Hydration of slag cement: Theory, modeling, and application, University of Twente (Doctoral Thesis), The Netherlands, 2007.

[31] F. Sajedi, H. Abdul Razak, Effects of thermal and mechanical activation methods on compressive strength of ordinary Portland cement–slag mortar. Mater. & Des. 32 (2011) 984-995.

[32] F. Sajedi, H. Abdul Razak, Thermal activation of ordinary Portland cement–slag mortars. Mater. Des. 31 (2010) 4522–4527.

[33] A. Sadrekarimi, Development of a light weight reactive powder concrete, J. Adv. Concr. Technol. 2 (3) (2004) 409–417.

[34] A. Bougara, C. Lynsdale, K. Ezziane, Activation of Algerian slag in mortars, Constr. Build. Mater. 23 (2009) 542–547.

[35] C.C. Castellano, V.L. Bonavetti, H.A. Donza, E.F. Irassar, The effect of w/b and temperature on the hydration and strength of blast furnace slag cements, Constr. Build. Mater. 111 (2016) 679–688.

[36] O.M. Abdulkareem, A. Ben, Fraj, M. Bouasker, A. Khelidj, Mixture design and early age investigations of an environmentally friendly UHPC, Constr. Build. Mater. 163 (2018) 235–246.

[37] M. Regourd, F. Gautier, Behaviour of concretes subjected to accelerated hardening (in French), J. Constr. Mater. 725 (1980) 240–248.

[38] M.H. Kazemi-Kamyab, Autogenous shrinkage and hydration kinetics of Sh-UHPFRC under moderate to low temperature curing conditions (Thesis), EPFL, 2013.

[39] P. Francisco, Déformations différées des bétons fibrés à ultra hautes performances soumis à un traitement thermique (Thesis), ENS Cachan, 2014 (in French).

[40] M. Ashraf, A.N. Khan, Q. Ali, J. Mirza, A. Goyal, A.M. Anwar, Physico-chemical, morphological and thermal analysis for the combined pozzolanic activities of minerals additives, Const. Build. Mater. 23 (2009) 2207–2213.

[41] N.E. Khalifa, M. Bouasker, P. Mounanga, N. Benkahla, Physico-chemical study of cementitious materials based on binary and ternary binders, Chem. Mater. Res. 4 (2013) 19–24.

[42] S. Kourounis, S. Tsivilis, P.E. Tsakiridis, G.D. Papadimitriou, Z. Tsibouki, Properties and hydration of blended cements with steelmaking slag, Cem. Concr. Res. 37 (2007) 815–822.

[43] M. Heikal, O.K. Al-Duaij, N.S. Ibrahim, Microstructure of composite cements containing blast-furnace slag and silica nano-particles subjected to elevated thermally treatment temperature, Constr. Build. Mater. 93 (2015) 1067–1077.

[44] C. Shi, D. Wang, L. Wu, Z. Wu, The hydration and microstructure of ultra high-strength concrete with cement-silica fume-slag binder, Cem. Concr. Compos. 61 (2015) 44–52.

[45] L. Rengguang, D. Shidong, Y. Peiyu, Microstructure of hardened complex binder pastes blended with slag, J. Chin. Ceram. Soc. 43 (5) (2015) 610–618.

[46] O.R. Ogirigbo, L. Black, Influence of slag composition and temperature on the hydration and microstructure of slag blended cements, Cem. Concr. Compos. 126 (2016) 496–507.

[47] S.N. Ghosh, Advanced in Cement Technology: Chemistry, Manufacture, and Testing, Tech Books International, New Delhi, India, 2002.

[48] A.A. Ramezannianpour, Cement Replacement Materials: Properties, Durability, Sustainability, Springer-Verlag, Berlin Heidelberg, Germany, 2014.

[49] C. Shi, D. Roy, P. Krivenko, Alkali-Activated Cements and Concretes, Taylor and Francis Group, USA, 2006.

[50] F. Collinsa, J.G. Sanjayan, Effect of pore size distribution on drying shrinkage of alkali-activated slag concrete, Cem. Concr. Res. 30 (2000) 1401–1406.

[51] S.L. Yang, S.G. Millard, M.N. Soutsos, S.J. Barnett, T.T. Le, Influence of aggregate and curing regime on the mechanical properties of ultra-high performance fibre reinforced concrete (UHPFRC), Constr. Build. Mater. 23 (2009) 2291–2298.

[52] R. Siddique, Waste Materials and By-Products in Concrete, Springer-Verlag, Berlin Heidelberg, 2008.

[53] K.V. Schuldyakov, L.Ya. Kramar, B.Ya. Trofimov, The properties of slag cement and its influence on the structure of the hardened cement paste, Proc. Eng. 150 (2016) 1433–1439.

[54] A. Gruskovnjak, B. Lothenbach, L. Holzer, R. Figi, F. Winnefeld, Hydration of alkali-activated slag: comparison with ordinary Portland cement, Adv. Cem. Res. 18 (3) (2006) 119–128.

[55] M. Heikal, M.Y. Nassar, G. El-Sayed, S.M. Ibrahim, Physico-chemical, mechanical, microstructure and durability characteristics of alkali activated Egyptian slag, Constr. Build. Mater. 69 (2014) 60–72.

[56] B.S. Gebregziabiher, R. Thomas, S. Peethamparan, Temperature and activator effect on early-age reaction kinetics of alkali-activated slag binders, Constr. Build. Mater. 113 (2016) 783–793.

[57] C. Bilim, C.D. Atiş, Alkali activation of mortars containing different replacement levels of ground granulated blast furnace slag, Constr. Build. Mater. 28 (2012) 708–712.

[58] D. Ravikumar, N. Neithalath, Effects of activator characteristics on the reaction product formation in slag binders activated using alkali silicate powder and NaOH, Cem. Concr. Compos. 34 (2012) 809–818.

[59] H. Yazıcı, M.Y. Yardımcı, H. Yiğiter, S. Aydın, S. Türkel, Mechanical properties of reactive powder concrete containing high volumes of ground granulated blast furnace slag, Cem. Concr. Compos. 32 (2010) 639–648.